ORIGINAL ARTICLE

Ethosomes-based gel formulation of karanjin for treatment of acne vulgaris: in vitro investigations and preclinical assessment

Sartaj Akhtar Ansari[1] · Abdul Qadir[2] · Musarrat Husain Warsi[3] · Mohd. Mujeeb[1] · Mohd. Aqil[2] · Showkat Rasool Mir[1] · Sanchit Sharma[1]

© King Abdulaziz City for Science and Technology 2021

Abstract

The aim of the present study was to develop and characterize karanjin-loaded ethosomes-based gel formulation for enhanced topical delivery and effective therapy of skin acne. Karanjin-loaded ethosomes (K-ETH) presented a nanometric size of 140.87 ± 2.35 nm, entrapment of $71.41 \pm 2.74\%$ and enhanced permeation with 1.9 times increase in the flux and 2.4 times higher skin deposition compared to the hydro-ethanolic solution of karanjin. The DSC analysis confirmed successful entrapment of the karanjin within the ethosomes. The developed ethosomes were incorporated in the carbopol gel for adequate application on the skin surface. The ethosomal gel (K-EGF) also exhibited greater penetration in the rat skin as revealed by CLSM. The optimized K-EGF formulation was non-irritant to the skin as evident by Draize score test and histopathological examination. The highest zone of inhibition, 30.0 ± 1.52 mm and 36.22 ± 0.57 mm was produced by the K-EGF against *Propionibacterium acnes* and *Staphylococcus epidermidis*, respectively, indicating substantial antibacterial properties of the K-EGF. DPPH assay indicated its potent antioxidant effects. Substantial anti-inflammatory effects in the carrageenan-induced edema in the rat paw were evident with inhibition of rat paw edema by 66.66% and 70.37% upon application of K-EGF and standard anti-inflammatory agent, respectively. Anti-acne effects were also evident with K-EGF treatment with significant decrease in number and size of sebaceous gland units in dermis. Overall, the above findings vouch for a therapeutic opportunity to improve topical delivery of karanjin in acne treatment employing ethosomal gels as the promising carrier system.

Keywords Acne vulgaris · Karanjin · Ethosomes · Anti-acne activity

Introduction

Acne vulgaris, a multifactorial pathology, has a prevalence of more than 85% in the teenagers and bears association with the exposome factors, including the nutritional, medical, psychosocial, occupational, climatic and lifestyle factors (Cong et al. 2019). Microbial fluctuation in the skin ecosystem contributes in acne pathogenesis. Bacterial species belonging to four phyla: *Actinobacteria*, *Proteobacteria*, *Bacteroidetes*, and *Firmicutes* are mainly present on the skin. Sebum and dead skin cells build-up within the sebaceous follicle enhances the microbial load which leads to the disruption of the follicular wall and also targets the keratinocytes and phagocytes, triggers the production of pro-inflammatory cytokines (interleukin (IL)-1β, IL-8, IL-12) and tumor necrosis factor-α and hence contributes to skin inflammation (Kumar et al. 2016). In addition to being a dermatologic disorder affecting the skin follicles in body parts like face, upper chest and back, acne severely affects

✉ Mohd. Mujeeb
  mohdmujeeb72@gmail.com

✉ Mohd. Aqil
  aqilmalik@yahoo.com

[1] Department of Pharmacognosy and Phytochemistry, Phytomedicine Laboratory, School of Pharmaceutical Education and Research, Jamia Hamdard, New Delhi 110062, India

[2] Department of Pharmaceutics, School of Pharmaceutical Education and Research, Jamia Hamdard, New Delhi 110062, India

[3] Department of Pharmaceutics and Industrial Pharmacy, College of Pharmacy, Taif University, Taif-Al-Haweiah 21974, Saudi Arabia

the social life, self-esteem and body image of the individuals, which may lead to psychological disorders leaving the individual in the state of depression and anxiety (Arora et al. 2011; Heng and Chew 2020). The symptoms of acne include development of non-inflammatory comedones with inflammatory lesions for instance papules, pustules, and nodules (Tanghetti 2013).

Acne development is influenced by four main pathological factors viz enhanced sebum production, irregular follicular desquamation, microbes, particularly *Propionibacterium acnes* (*P. acnes*) proliferation and inflammation of the area (Gollnick et al. 2003). Treatment for acne includes systemic and topical therapies with retinoids, antibiotics, hormonal treatment and also physical treatment which includes extraction of comedone, cryo-slush therapy, electro-cauterization, intra-lesional corticosteroids and optical therapy (Fox et al. 2016). However, most of the products are inadequate to control all the pathogenic factors contributing to acne disease. The associated side effects, such as skin irritation, dryness, teratogenicity, photosensitivity and antibiotic resistance, are other concerns for acne treatment (Yu et al. 2016). This necessitates development of alternative treatment for acne.

Herbal therapies, such as herbal extracts, oils and ayurvedic formulations, have been used since ages for disease treatment and also explored for their anti-inflammatory action in acne lesion. The antibacterial and the anti-inflammatory actions of the natural substances have led to their potential use in acne treatment (Azimi et al. 2012; Kumar et al. 2008; Shahtalebi et al. 2018; Yang et al. 2019). *Pongamia pinnata* L. Pierre (Fabaceae; synonym *Pongamia glabra* Vent.), is a frequently utilized traditional Indian medicinal plant possessing antitumor, anti-ulcerogenic, anthelmintic, anti-inflammatory, analgesic and anti-oxidative properties. It is also used in various skin disorders and also for the treatment of bronchitis, chronic fever and rheumatism (Yi et al. 2015). Karanjin, a major bioactive furanoflavone, obtained from *P. pinnata* seeds has demonstrated potential antioxidant, anti-inflammatory and H$^+$, K$^+$-ATPase inhibitory effects (Shejawal et al. 2014). Reduced secretion of inflammatory mediators and inhibition of nitric oxide are some of the inflammation inhibiting effects of karanjin (Patel and Trivedi 2012; Singh and Pandey 1996; Srinivasan et al. 2001). Potent antioxidant effects of karanjin were observed through nitric oxide-scavenging ability (Ghosh and Tiwari 2018). Karanjin also produces the antimicrobial effect against *Pseudomonas aeruginosa*, *Klebsiella pneumonia* and *Micrococcus luteus* (Rani et al. 2013). Treatment with karanjin produced some morphological changes, such as shrinking, membrane disruption and break down of the cell wall in the bacterial strain of *Staphylococcus aureus* and *Escherichia coli* enterotoxin (Singh et al. 2016; Ujwal et al. 2007). Karanjin

is therefore a valuable antioxidant with promising prospects. Considering the potential antioxidant, anti-inflammatory and antibacterial activity of karanjin, it can be plausibly explored for the treatment of acne vulgaris.

Despite promising benefits with topical delivery systems, a potential challenge in acne treatment is drug penetration through the deeper layers of the skin due to defensive membrane structure of the stratum corneum (SC). Formulating elastic vesicles such as ethosomes owing to their soft and malleable nature can penetrate the deeper layers of skin (Garg et al. 2017).

Ethosomes are squishy, delicate and pliable vesicles altered for enhanced delivery of therapeutic agents. These are phospholipid-based nano-vesicles containing ethanol at high percentages (20–45%) which imparts flexibility to the vesicular membrane, hence allowing their transport through pores of very small diameters (Yu et al. 2016). The presence of ethanol in the ethosomes causes the perturbation of multi-lamellar and ordered lipid domain, reduces the structural density and increases the fluidity of the SC, thereby promoting percutaneous permeation of the therapeutic agent into the deeper skin layers. Moreover, a steady-state flux can be attained throughout the skin in contrast to liposomes as the latter is largely confined to the upper tier of SC (Bragagni et al. 2012). Additionally, the fusion of the ethosomal vesicle with the SC lipid contents results in change of the transition temperature and hence enhanced drug diffusion (Kahraman et al. 2017). Ethosomes have number of features that make them ideal for use as drug carrier, including a smaller size as compared to liposomes; with similar lipid composition, high payload for both lipophilic and hydrophilic therapeutics and have great physical stability during storage (Touitou et al. 2000). Ethosomes have been widely explored as scaffold for several drugs used in therapy of hair disorders and diseases associated with sebaceous gland, photodynamic therapy, and delivery of anesthetics (Yang et al. 2017).

Considering the involvement of pathogenic factors, such as oxidative stress, inflammation and bacterial proliferation, in the pathogenesis of acne vulgaris, we aimed to explore the potential antioxidant, antibacterial, anti-inflammatory to investigate anti-acne effect of karanjin-loaded ethosomes and ethosomal gel. The antibacterial efficacy of the developed ethosomes and ethosomes-loaded carbomer gel was tested against acne-causing bacteria, *P. acnes* and *Staphylococcus epidermidis* (*S. epidermidis*). The antioxidant activity was assessed via DPPH assay. In vivo pharmacodynamic evaluation was performed in carrageenan-induced edematous rats for the anti-inflammatory effect and testosterone-induced sebaceous gland enlargement for evaluation of anti-acne effect.

Materials and methods

Materials

Karanjin was purchased from Yacca Enterprises Mumbai. Phospholipid 90G and Carbopol 934 were obtained from B.S. Goodrich, Cleveland. Chloroform, methanol (HPLC grade), triethanolamine, methyl paraben of AR category were purchased from S.D. Fine Chemicals Ltd (Mumbai, India). Testosterone (Testoviron depot inj. 100 mg/ml) was procured from Zydus cadila Health Care Ltd. Clindamycin containing marketed formulation (0.5% gel) and standard herbal cream were procured from Alkem Laboratories Ltd, Mumbai and Himalaya Drug Company, Makali, Bengaluru, respectively. Test organisms *Staphylococcus epidermidis* (*S. epidermidis*) (MTCC 435) and *Propionibacterium acnes* (*P. acnes*) (MTCC 1951) were obtained from the Microbial Type Culture Collection and Gene Bank (MTCC), Chandigarh. Typical soy broth (TSB) and Modified brain heart infusion medium were obtained from Himedia, India. Double-distilled water was used throughout the study.

Preparation of ethosomes

Ethosomes were prepared according to the film hydration method (Dubey et al. 2007). Phospholipids 90G (30 mg, w/w) and drug Karanjin (3% w/v) were weighed accurately and dissolved in chloroform: methanol (2:1, v/v). The mixture was evaporated in a rotatory evaporator (HAHN SHIN, HS-2005V-N) at 200–250 rpm and exceeding the transition temperature of the phospholipids to obtain a thin film. Removal of traces of solvent was carried out overnight under vacuum. Hydration of the obtained thin film was done using isotonic phosphate buffer:ethanol solution (25:75) above the lipid transition temperature for 1 h. The vesicular suspension was dispersed using probe sonicator (Heilscher Ultrasonics, UP 50 H; Germany) at 50% amplitude for 5 min. The obtained karanjin-loaded ethosomes (K-ETH) were stored in refrigerator until further use.

Evaluation of ethosomes

Vesicle size and size distribution analysis

The vesicle size and polydispersity index (PDI) were measured by dynamic light scattering (DLS) at the angle of 90° employing a computerized assessment system (Nano ZS90, Malvern instrument, UK). All the samples were diluted with deionised water before the size measurements. Determinations were made in triplicate and at temperature of 25 °C.

Determination of entrapment efficiency

The encapsulation of karanjin in vesicles system was investigated using centrifugation method. Vesicles suspensions (1 ml) were centrifuged at 15,000 rpm for 30 min. Following centrifugation, the supernatant and pellet were separated, and the concentration of karanjin was analyzed by HPLC Method. The entrapment efficiency was calculated using the following equation:

$$\%EE = \frac{\{T - S\}}{T} \times 100, \tag{1}$$

where T represents the total drug found in both the sediment and supernatant while S refers to the amount of drug presented in the supernatant (Godin and Touitou 2004).

Vesicular shape and surface morphology

Transmission electron microscopy (TEM) was performed using TEM (Philips CM 12 Electron Microscope, Eindhoven, Netherlands) for assessing the vesicular shape. Sample (K-ETH) was placed on carbon-coated grid, dried and negative staining was performed using aqueous solution of Phosphotungstic acid. The dried specimen was observed using the TEM. For the scanning electron microscopy (SEM) study, sample of K-ETH was put on the glass stub, dried, coated with Polaron E 5100 Sputter coater (Polaron, UK) and examined using SEM (Leo-435 VP, Cambridge, UK).

Differential scanning colorimetry (DSC) analysis

Differential scanning colorimetry (DSC) analysis was performed for investigation of the physical state of drug and excipients when entrapped within the ethosomal vesicles. Transition temperature (T_m) of the samples was analyzed using Mettler DSC 60 equipped with Mettler Toledo Star software (Mettler, Switzerland). Samples including standard karanjin, physical mixture and freeze-dried ethosomes (K-ETH) were scanned at a range of temperature (30–250 °C) with a heating rate of 10 °C/min, under a constant flow of nitrogen gas.

Ex-vivo permeation studies

Modified Franz diffusion cell apparatus was employed to study the permeation of karanjin through rat skin.

Skin source and preparation of skin

Skin was obtained from male Wistar albino rats (150–200 g) acquired from animal house facility at Jamia Hamdard. All the procedures applied in this study were in accordance with the institutional guidelines. Dorsal hairs of the excised skin from the abdominal region were removed with the help of an electrical clipper and subcutaneous fat was removed by treating the excised skin with isopropyl alcohol. The skin was finally washed with distilled water, observed physically for any damage, stored at -21 °C and used within a week.

The skin was cut to appropriate size, sonicated and applied over the receptor compartment and kept for magnetic stirring at 200 rpm. The temperature of the system was maintained at 37 ± 0.5 °C. The skin was stabilized for 4–5 h with replacement of buffer solution at regular intervals.

Permeation studies

Vertical diffusion cells (diffusion area 1.766 cm^2; receiver capacity, 12.2 ml) were used for in vitro permeation experiments. Phosphate buffer (pH 7.4) with 1% sodium lauryl sulfate was used as the receptor medium. The receptor cell was filled with the media and K-ETH (1 ml) was placed on the skin fitted between the two half cells with SC facing the donor compartment. The receptor medium was maintained at 37 ± 0.5 °C and magnetically stirred at 200 rpm. 1 ml of the receptor media was collected at regular intervals (initial and 0.5–12 h) with sampled volume being replenished by fresh medium. Karanjin concentrations were analyzed using HPLC (Ravikumar et al. 2011).

Cumulative amount of drug permeated per unit area (µg/cm^2) was calculated at the end of 12 h of study. A graph was plotted between amount of drug permeated vs. time. The flux was calculated as the slope of the above graph.

$$\text{Permeability coefficient } (K_p) = \frac{\text{Flux}}{\text{Initial drug concentration } (C_0)}. \tag{4}$$

At the end of the study, the skin was removed, cleaned, weighed, and sonicated with methanol to extract karanjin. The resulting solution was centrifuged and karanjin concentration (µg/mg of skin) was analyzed by HPLC.

Fabrication of ethosomal gel

The optimized ethosomal formulation was selected for the preparation of karanjin-loaded ethosomal gel (K-EGF), an anti-acne gel with 3% concentration of karanjin. A 1.5% (w/v) Carbapol 934 gel was prepared and neutralized using triethanolamine (0.05%, v/v). Preservative, methyl paraben was added to the gel. The colloidal ethosomal suspension (K-ETH) (10 ml each) was mixed with propylene glycol and added to the Carbopol 934 solution slowly with continuous stirring until homogenous. Conventional hydro-ethanolic gel loaded with karanjin (at equivalent concentrations) (K-CGF) was also prepared as a control.

Evaluation of ethosomal gel

The optimized gel pH was evaluated using pH meter (Mettler Toledo, MP 2020 (Mumbai, India). The developed gel was examined visually for homogeneity for its appearance and existence of any aggregates after the gel has been set in the container.

The viscosity of the gel preparation was established at room temperature using Vicostar viscometer (Fungilab S.A., Spain). The measurements were made using spindle number 5 at 2 rpm.

Texture profile analysis (TPA) was done by employing a TAXT PLUS Texture Analyzer (Stable Microsystem, Surrey UK). Formulation (50 g) was transferred into a standard size back extrusion container. The extrusion disk was positioned centrally over the sample container. A probe (cylindrical) with diameter of 35 mm was driven downward into the sample at a rate of 2 mm/s and up to a

$$\text{Amount of drug permeated} = \frac{\text{Concentration}\left(\frac{\mu g}{\text{ml}}\right) \times \text{volume of diffusion cell}}{\text{Area}\left(\text{cm}^2\right)}, \tag{2}$$

$$\text{Flux} = \text{Slope of steady state portion of the plot between amount of drug permeated per cm}^2 \text{ vs time}\left(\frac{\frac{\mu g}{\text{cm}^2}}{\text{h}}\right), \tag{3}$$

depth of 30 mm. From the resulting force–time plots, the firmness, consistency, index of viscosity, cohesiveness and work of adhesion were derived.

Spreadability of the developed gel (K-EGF) was analyzed by wooden block and glass slide system. K-EGF (approximately 20 g) was placed on the pan and the time for upper slide (moveable) to separate completely from the fixed slides was noted (Fang et al. 1999). Spreadability was determined by employing the below formula:

$$S = \frac{M \times L}{T}, \tag{5}$$

where M is weighed tide to upper slide, L is glass slide length and T is total time to split the slide entirely from each other.

Consistency of the developed K-EGF was evaluated using the method of William et al. 2000 (Remington, 2006). Penetration of the cone when dropped into the glass cup center filled with K-EGF was determined. The distance traveled by cone was recorded after 60 s.

Permeation studies of karanjin from K-EGF were also performed as per the protocol described under Sect. 2.4. Comparison was made between the K-EGF and the K-CGF.

Assessing depth of permeation using confocal microscopy

The optimized gel formulation (K-EGF) and 0.05% w/v hydro-alcoholic solution of Rhodamine B dye were applied homogeneously to the excised rat skin installed on the Franz diffusion cell for 8 h. The skin was then removed and a slide was made which was observed under confocal microscope (Leica TCS Spectral CLSM 710, UK) with excitation at 488 nm and emission at 590 nm.

Skin irritation studies

Visual method

Skin irritation potential of the anti-acne K-EGF was investigated using Draize Score test (Draize 1944). Two specific areas on the interscapular region of the Wistar albino rats ($n=3$) were shaven off and one part was kept intact while other was slightly abraded. K-EGF (0.3 g) was applied for 24 h. The skin reaction was evaluated on the basis of scale weighted score post 24 h upon removal of the gel and observed for additional period of 72 h. The average of the reading at 24 h and 72 h was noted.

Scores of 0–4 were given based on the degree of erythema (redness) and edema (swelling): 0 indicates no erythema and edema, score 1 is given to slight erythema and edema, 2 for moderate erythema and edema, 3 for moderate

to severe erythema and edema, and 4 to severe erythema (extreme redness) and edema (extreme swelling).

Histopathological examination

The Wistar albino rats ($n=3$) were shaven off from the interscapular region using a mechanical hair clipper and treated with K-EGF twice a day for two consecutive days. After 48 h, rats were sacrificed and the skin from the treated area and adjacent untreated area (control) was taken. Each section was conserved in 10% formalin solution. The skin specimens were cut into sections vertically, and were mounted on glass slides. The samples were visualized under optical light microscope (Motic, Japan) and assessed for any skin irritation effects (Draize 1944).

Pharmacological activity

Prepared Ethosomal gel (K-EGF) was subjected to various pharmacological activities including: (a) Anti-bacterial activity, (b) Anti-oxidant activity, (c) Anti-inflammatory studies and (d) Anti-acne activity (on sebaceous glands).

Antibacterial activity against acne-causing bacteria

The antibacterial activity of K-EGF, standard allopathic gel (Clindamycin containing marketed formulation (0.5% gel) (Std. allopathic), marketed herbal preparation (Himalaya) (Std. herbal) and *Pongamia pinnata* L. (dried seeds) extract (PP extract) was evaluated using modified agar well diffusion method (Chomnawang et al. 2005). The inocula of *S. epidermidis* and *P. acnes* were made by incubating in tryptic soy broth at 37 °C for 24 h for *S. epidermidis* and in modified brain heart infusion medium (MBHI) for 48 h under anaerobic condition for *P. acnes*. The prepared inoculum was added to the nutrient agar, mixed, poured over the surface of the agar base and left to solidify. Test solutions (200 µl) were added into the 8 mm wells prepared in nutrient solidified agar plates and incubated at 37 ± 1 °C for 24 h under anaerobic conditions and diameter of zones of inhibition (in mm) was measured.

Anti-oxidant activity

The DPPH free-radical scavenging activity of K-ETH was evaluated using a specific HPLC method (Chandrasekar et al. 2006). Stock solutions of DPPH (2.5 mM/ml) and the standard antioxidant Butylated Hydroxyanisole (BHA) (1 mM/ml) were prepared in methanol. K-ETH (at different concentrations) were diluted in methanol. Equal amounts (100 µl) of different concentrations of standard antioxidant or ethosomal formulation in methanol were added to 100 µl

of DPPH solution (final concentration 250 μM/200 μl), vortexed and allowed to stand in dark at room temperature for 20 min.

The samples were subjected to HPLC analysis. The reversed-phase HPLC system consisted of a Shimadzu HPLC (LC-10 Ai, Japan) with a diode array detector (SPD-M10 AVP) equipped with class LC10 software (Version 1.6) was employed. Chromatographic separation was carried out on a LiChrospher® 100RP-C18 Column (250 mm × 4 mm, 5 μM) (Merck, Darmstadt, Germany) using methanol:water (80:20, v/v) as the mobile phase at a flow rate of 1 ml/min. The DPPH peaks were observed at 517 nm and the percent radical scavenging activity of the sample was calculated using the formula:

$$\text{Radical scavenging (\%)} = \left\{ \frac{PA_{BLANK} - PA_{SAMPLE}}{PA_{BLANK}} \right\} \times 100, \tag{6}$$

where PA_{BLANK} is the peak area of blank, PA_{SAMPLE} is the peak area of sample.

Anti-inflammatory studies

Experimental animals

The study was approved by Institutional animal ethics committee (IAEC) (Approval number: 1400). Wistar rats (120–200 g) were obtained from the central animal house facility, Jamia Hamdard. All animals were kept in standard conditions and fed with standard rodent food with free access to water.

Carrageenan-induced rat paw edema

The inhibitory effect of the K-EGF on Carrageenan-induced edema was evaluated using method of Yesilada (2002) with some modifications (Yeşilada and Küpeli 2002). Before the trial, the animals were fasted for 24 h and given free access to water. Approximately 50 μl of Carrageenan suspension (1%) in saline (CGN*) was injected into the plantar side of right hind paw of rat. Animals were divided into four groups and received the following treatments: Group 1 served as the normal control, Group 2 was the vehicle control group and received CGN* + blank Ethosomal gel (Blank-EGF), Group 3 received CGN* + standard anti-inflammatory gel (Clindamycin containing marketed formulation (0.5% gel) (Std. anti-inflammatory), Group 4 received CGN* + anti-acne gel containing 3% karanjin. The formulations were applied 1 h prior to the CGN* injection. Paw volume was measured immediately after CGN* injection and at intervals of 1, 2 and 3 h using a Plethysmometer (Model 7159, Ugo Basile arese, Italy).

$$\%\text{Inhibition} = \frac{(D_t - D_0)\text{Control} - (D_t - D_0)\text{test} \times 100}{(D_t - D_0)\text{Control}}, \tag{7}$$

where D_t is the linear paw circumference at 3 h after CGN* Inj, D_0 is the linear paw circumference at 0 h just before CGN* Inj.

Anti-acne activity (on sebaceous glands)

For the anti-acne activity evaluation, animals were divided into groups of 5 ($n = 5$). Group 1 was the normal control group, Group 2 was the toxic control group which received the testosterone injection (im) (1.42 mg/kg), Groups 3, 4 and 5 were given Std. allopathic, Std. herbal and K-EGF, respectively. Interscapular area of the rats was shaved off and Testosterone injection (im) was given daily to the animals of all groups except normal control for 14 days. On 14th day, the skin was excised from the normal control group and the toxic control group and subjected to histopathological analysis to verify the sebaceous glands (SG) enlargement in toxic group. Post confirmation of SG enlargement, the test preparations were employed in the vicinity of the shaved area at increasing doses (0.05, 0.5, and 5 mg/cm^2) to the animals of respective groups. The treatment was continued for 7 days. The animals were sacrificed after 24 h of the last treatment and skin was processed for histopathological examination.

Accelerated stability studies

Stability testing was carried out for 3 months as per ICH guidelines at a temperature of 40 ± 2 °C and relative humidity (RH) $75 \pm 5\%$ (International Conference on Harmonization 2003). All the gel formulations were observed for the change in appearance, pH and drug content using HPLC Method.

Statistical analysis

Statistical analysis was done using GraphPad Prism software (v 5.03, San Diego, CA, USA) with one-way analysis of variance (ANOVA), followed by Dunnett's test (compare all vs. control) to determine the statistical significance of the data. All values are presented as mean $\pm$ standard deviation (S.D.). Statistical significance was considered at p value less than 0.05.

Results and discussion

Karanjin-loaded ethosomes (K-ETH) were prepared using the film hydration method. Preliminary experiments (data not shown) were conducted to define the optimized conditions for the preparation of ethosomes. Smaller-sized ethosomes with optimal entrapment of karanjin could be observed with phospholipid concentration of 30 mg (%w/w), ethanol:buffer ratio of 25:75 and produced with

5 min sonication. Higher amounts of lipid are required for the higher entrapment efficiency as a higher lipid concentration provides greater capacity to accommodate the drug in the inner core which may be due to higher carrying capacity of the phospholipid molecules and solvent effect (Garg et al. 2016; Kausar et al. 2019). However, amount of phospholipid used needs to be regulated as higher lipid fraction can lead to increased vesicular size which can be ascribed to the formation of highly thickened matrix structure. Optimal ratios of ethanol are desirable as too high concentrations can cause reduction in the thickness of bilayer membrane, making them leaky or may lead to interpenetration of the ethanol hydrocarbon chain which can reduce the particle size and decrease in entrapment efficiency of system. Similarly, at low ethanol concentrations, drug entrapment will be minimal (Abdulbaqi et al. 2016). Fang et al. stated that net charge of the vesicles could be altered by ethanol, resulting in some steric stability and a reduction in size of vesicle (Fang et al. 2008). Sonication time also influences the development of small-sized ethosomes. Increasing sonication time up to a certain limit leads to a decrease in particle size; however, with higher sonication time, a gradual increase in vesicular size was observed. A decrease in entrapment efficiency is observed with higher sonication time which is due to increased acoustic cavitation provided by the sonication (Negi et al. 2013).
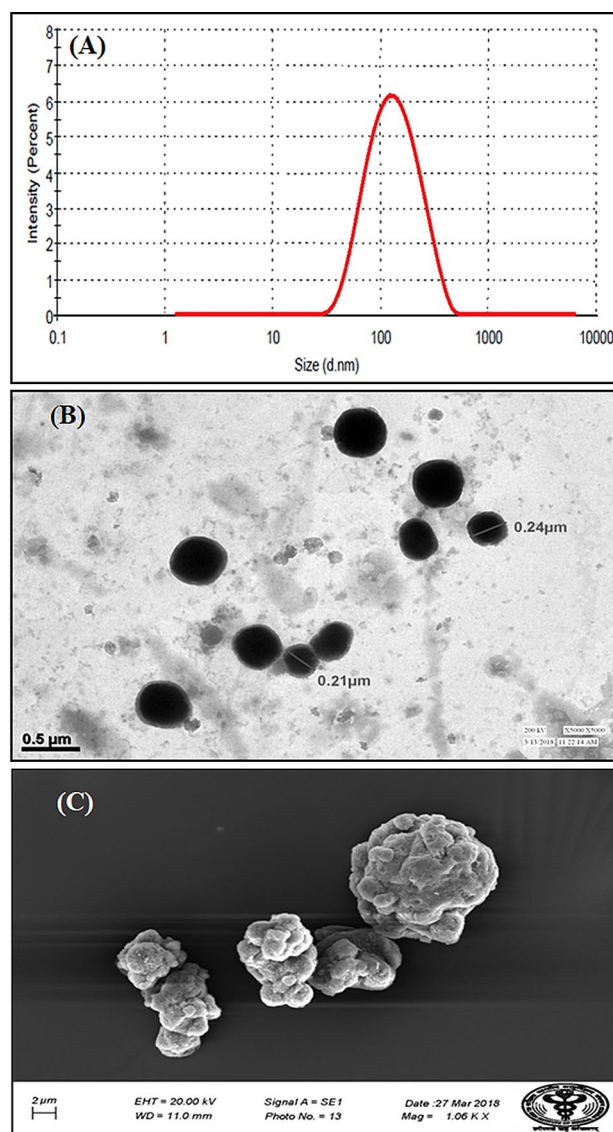
Characterization of karanjin-loaded ethosomes (K-ETH)

Assessment of vesicle size and entrapment efficiency and morphological characterization

K-ETH produced a particle size of 140.87 ± 2.35 nm (Fig. 1A), polydispersity index (PDI) of 0.168 ± 0.012 and sufficient entrapment of $71.41 \pm 2.74\%$. The electron microscopy images of the optimized formulation revealed vesicles of spherical shape and smooth morphology with fine distribution in the nano-range (Fig. 1B, C). Vesicles' size of less than 300 nm is critical for penetration of payloads into the deep layers of the skin via topical route (Yu et al. 2016). The developed ethosomes were within the size range and hence have potential for karanjin delivery deep into the skin.

Differential scanning colorimetry (DSC) analysis

Differential scanning colorimetry (DSC) thermograms of standard karanjin, physical mixture of karanjin and excipients and freeze-dried K-ETH are presented in Fig. 2. A

Fig. 1 Particle size and size distribution (**A**) morphological characterization; TEM Microphotograph (**B**) and SEM microphotograph (**C**) of karanjin ethosomes (K-ETH)

sharp endothermic peak of karanjin could be observed at 156.8 °C corresponding to its melting point (Fig. 2A). A similar endothermic peak at 156.9 °C was also seen in the physical mixture which indicated least interaction between the drug and the excipients (Fig. 2B) In contrast, a reduced peak of karanjin with area under the peak of 26.48 mJ and enthalpy change, delta H value of 26.84 J/g was observed (Fig. 2C) in case of ethosomal formulation (K-ETH) which implied change in the drug crystalline state or molecular dispersion of karanjin in the lipid matrix (Ahmed 2015).
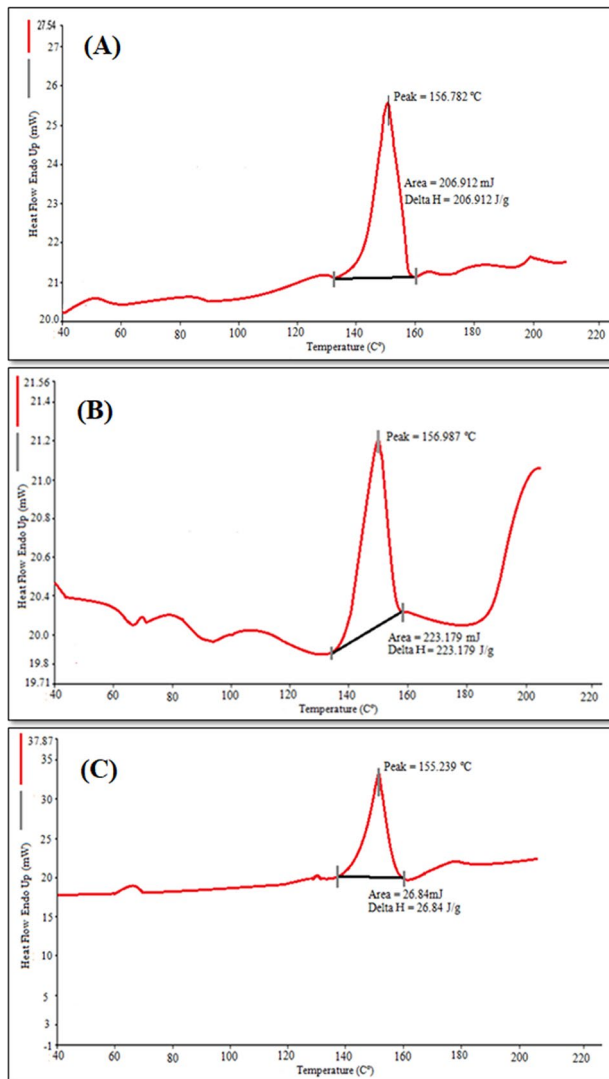
Fig. 2 DSC Thermograms of (**A**) Standard karanjin, (**B**) Physical mixture of karanjin and excipients, (**C**) karanjin-loaded ethosomes (K-ETH)

Ex-vivo permeation studies and drug retaining on skin surface

The permeation properties of K-ETH and hydroethanolic solution of karanjin (K-HES) were represented by cumulative amount of karanjin permeated per unit area (µg/cm^2) plotted as a function of time (Fig. 3A). Transdermal flux (33.28 and 62.84 µg/cm^2/h for K-HES and K-ETH, respectively) and permeability coefficient (1.10×10^{-3} and 2.09×10^{-3} cm h^{-1}) were higher for ethosomal formulation compared to the hydro-ethanolic solution, while 0.7 and 1.68 µg/mg drug were retained on the skin. Ethosomes exhibited approximately 1.9 times increase in the flux when compared to the K-HES which indicated the potential of ethosomes as effective dermal delivery vesicles.
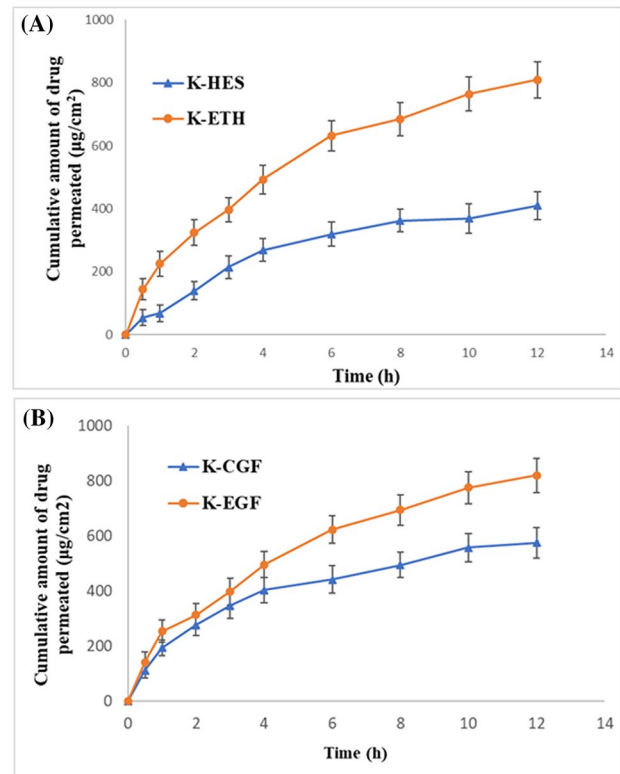
Fig. 3 Permeation profile of (**A**) karanjin from hydro-ethanolic solution (K-HES) and ethosomal formulation (K-ETH); (**B**) Karanjin from conventional gel (K-CGF) and ethosomal gel (K-EGF)

Furthermore, deposition of karanjin into skin by the ethosomes was 1.68 µg/mg which was about 2.4 times higher than the solution form of karanjin which showed that the ethosomes increased the deposition of karanjin into skin. The enhanced permeation properties with the ethosomes can be related to the synergistic interplay of ethanol as penetration enhance with skin lipids and vesicles. Ethanol fluidizes both the vesicular and SC lipids providing greater flexibility and enhanced permeation while phospholipids aid in vesicles mixing with the skin lipids developing openings in the SC for ease of drug penetration (Ibrahim et al. 2019). Chin and Goldstein (1997) reported that blending of intercellular layers SC lipids with vesicles lipids further boosts the skin permeability of drugs, which further supports the outcomes of our permeation study.

Fabrication of anti-acne ethosomal gel

The ethosomal dispersion of karanjin possessed low viscosity indicating inadequate application to the skin surface and hence lack of patient compliance. Therefore, to improve the consistency of the final dosage form, a 1.5% w/w Carbopol 934 gel was incorporated with the optimized ethosomes. The

developed ethosomal gel was slightly yellowish in color, translucent and smooth and slippery to touch.

Characterization of ethosomal gel

Different parameters were assessed for the karanjin-loaded ethosomal gel (K-EGF). The pH of the prepared gel was 6.8 ± 0.08 indicating that the gel was non-irritant to skin. The content of karanjin in the ethosomal gel was found to be $99.39 \pm 0.44\%$, indicating non-significant drug loss during the gelling process. Texture profile analysis is crucial for a topical formulation as it is associated with the stickiness, ease of application and overall acceptance of the product (Hurler et al. 2012). K-EGF showed good homogeneity with no lump formation. The non-sticky nature of the K-EGF was supported by several parameters including hardness (118.44 g), firmness (108.61 g), index of viscosity (− 580.72 g s), cohesiveness (− 74.20 g) and consistency (936.55 g s) (Fig. 4). The spreadability value of 6.58 ± 0.33 g.cm/sec and adhesiveness value − 259.909 g s indicate that the gel was easily spreadable by small amount of shear, was free from severe adhesion and required minimal force and work of adhesion. The observed characteristics of the ethosomal gel fulfilled the ideal requirements of the topical gels for dermal applications.

Permeation studies of karanjin-loaded ethosomal gel

Cumulative amount of karanjin permeated from the gel was plotted against time to calculate the permeation parameters (Fig. 3B). The flux value of K-EGF (63.32 µg/cm^2/h) was higher than that of K-CGF (42.56 µg/cm^2/h). The permeability constant (Kp) was found to be 1.62×10^{-2} and 2.36×10^{-2} for K-CGF and K-EGF, respectively. This indicated greater

permeation of karanjin across the skin from the developed ethosomal gel. Furthermore, maximum drug was retained in the skin with the K-EGF (0.89 µg/mg) compared to K-CGF (0.57 µg/mg).

Assessing depth of permeation using confocal microscopy

The penetration depth of ethosomal gel formulation (K-EGF) in the rat skin was studied using confocal microscopy and was compared with the hydro-alcoholic solution of rhodamine B. Figure 5 showed the intensity of rhodamine red fluorescence at various depth of skin and the fluorescence intensity is correlated with the density of each formulation permeated into the skin. The intensity was highest at 0.0 µm, i.e., on the surface of the skin and decreased with the depth of skin and became negligible after 64.9 µm and 44.9 µm upon treatment with K-EGF and standard gel, respectively. This can be ascribed to the combined "ethanol effect" and the "ethosome effect" which leads to enhanced delivery of rhodamine in terms of depth and quantity along with the ethosomal gel formulation (Verma and Pathak 2012).
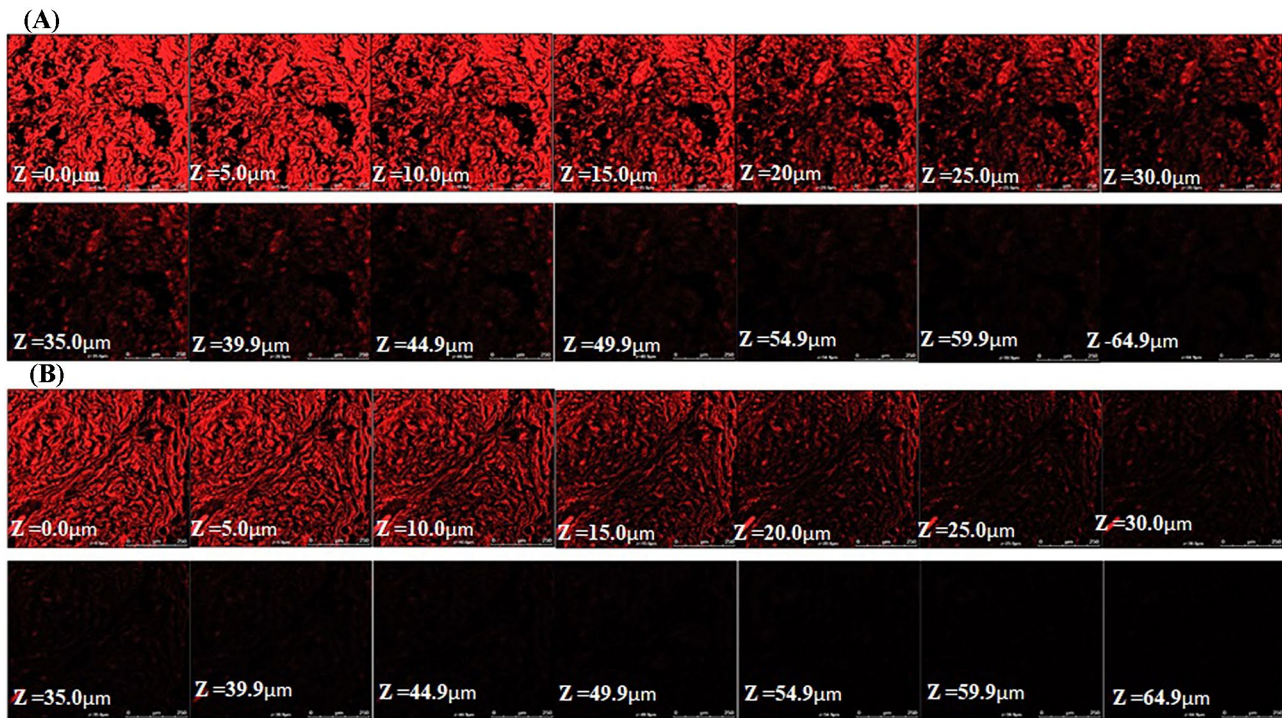
Skin irritation studies

Visual Method

Skin irritation capability of K-EGF was evaluated using Draize test. Substances with score of 2.00 or less are regarded as non-irritants (Draize 1944). The skin irritation score of K-EGF was 1.73, which indicated non-irritant nature of the prepared gel.

Fig. 4 Texture profile analysis of karanjin-loaded ethosomal gel (K-EGF)

(A)

(B)
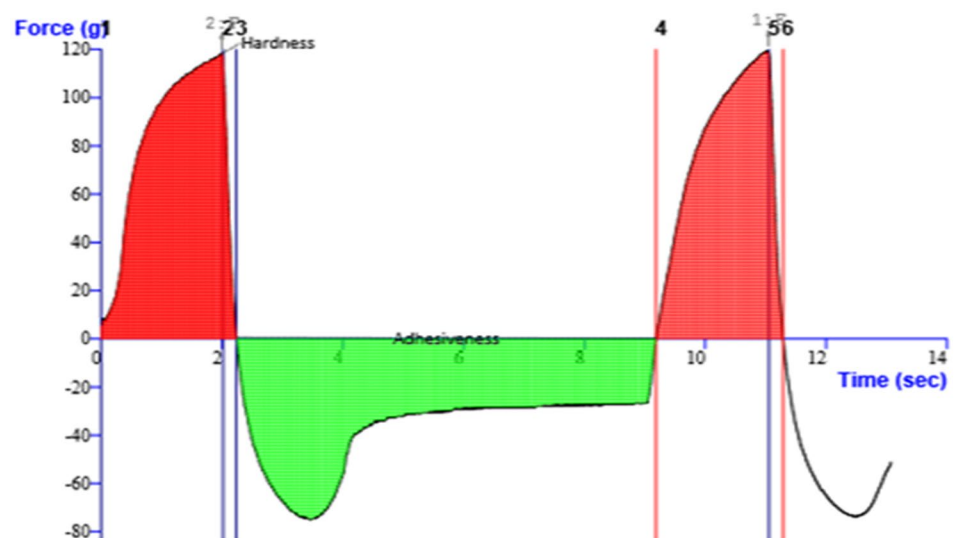
Fig. 5 Confocal laser scanning micrographs (CLSM) of (**A**) rhodamine-loaded ethosomal gel and (**B**) hydroalcoholic solution of Rhodamine B, with a difference of 5 μm that is from 0 to 70 μm depth

Fig. 6 Photomicrograph of section of (**A**) untreated rat skin (control) and (**B**) treated rat skin with optimized ethosomal gel formulation (K-EGF)
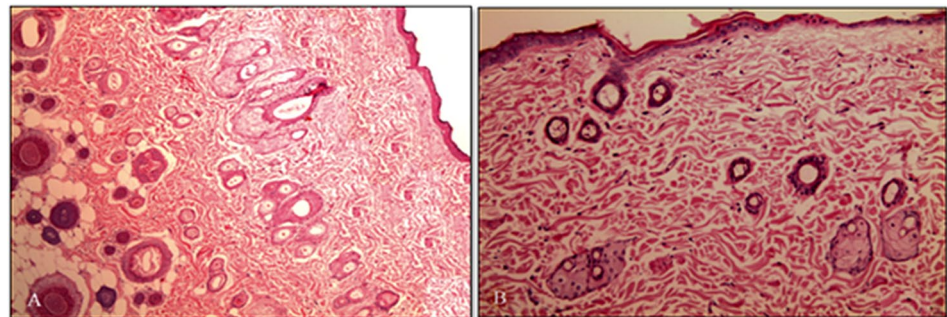
Histopathological examination

Figure 6A, B showed the photomicrograph of the rat inter-scapular region of the control (untreated) skin and K-EGF treated skin, respectively. Well-defined epidermal and dermal layers were evident in the control group with SC presented as a layer of individual keratinized cells (cor-neocytes) peppered in lipid areas. Upon treatment with K-EGF, the skin produced distinct changes in keratinized layer which are due to the action of permeation enhancer (ethanol) on the keratinized cells of SC only (Horita et al. 2015). Dermis and skin appendages remained intact. This suggested that the K-EGF was devoid of any skin irritation.

Pharmacological studies

Antibacterial activity against acne-causing bacteria

The antibacterial activity of K-EGF was compared with standard allopathic gel (Clindamycin containing marketed formulation (0.5% gel) (Std. allopathic, Clindac A gel), marketed herbal preparation (Std. herbal) and *Pongamia pinnata* L. (dried seeds) extract (PP extract) against acne-causing bacteria *P. acnes* and *S. epidermidis*. The K-EGF displayed highest antibacterial activity as evident with greater zone of inhibition (30.0 ± 1.52 mm), compared to Std. allopathic (22.76 ± 1.52 mm), Std. herbal

(13.33 ± 1.52 mm) and PP extract (14.21 ± 1.04 mm) against *P. acnes* and 36.22 ± 0.57 mm, 28.89 ± 1.00 mm, 15.13 ± 1.73 mm and 18.43 ± 1.15 mm zone of inhibition observed with K-EGF, Std. allopathic, Std. herbal and PP extract, respectively, against *S. epidermidis*. It was confirmed that K-EGF had greater antibacterial activity against acne-causing bacteria as compared to other standard preparations. *P. acne* is the crucial target for antibacterial treatment in acne vulgaris. *P. acnes* proliferation is favored by retention of sebum which is due to impediment of the follicular canal by the abnormal desquamation of the follicular epithelium. It further produces different inflammatory substances that induce the development of inflammatory lesions (Dreno 2004). Therefore targeting *P. acne* can reduce bacterial load and inflammation in acne vulgaris.

Antioxidant activity evaluation

The anti-oxidant activity for K-ETH was evaluated using the simple and sensitive HPLC technique. The HPLC method used was specific for DPPH with a low run time, letting quick analysis of radical scavenging activity (%) of several samples (Supplementary Table 1). It was observed that the K-ETH at a concentration of 100 µg/ml had scavenging activity of 63.10% which was analogous to that of the standard BHA (100 µg/ml) (66.18%). The radical scavenging activity of the K-ETH was increased with the increase in its concentration. The higher antioxidant effects with K-ETH can be ascribed to the antioxidant activity of karanjin (Arshad et al. 2013; Ghosh and Tiwari 2018). The ethosomal formulation showed strong free-radical scavenging activity, which is an ideal requirement for anti-acne formulation. Oxidative stress and inflammation also contribute to the pathogenic factors leading to acne. Reactive oxygen species (ROS) production by neutrophils can damage the follicular wall to cause lipid peroxidation that reduces the important skin antioxidant, reduced glutathione (GSH) and initiates an inflammation cascade, stimulating the inflammatory cytokine production. Furthermore, oxidative stress within the pilosebaceous unit alters the oxygen concentration in the

follicle making it suitable for the colonization of anaerobic bacteria such as *P. acnes*. Antioxidant intervention is therefore crucial for acne management (Wong et al. 2016).

Anti-inflammatory studies

The anti-inflammatory effect of the developed gel (K-EGF) and standard anti-inflammatory agent (Clindamycin containing marketed formulation gel) was evaluated in Carrageenan-induced edema model. The K-EGF produced a comparable reduction of swelling of the rat paw edema with % inhibition of 66.66% compared to the Std. anti-inflammatory agent (70.77%) (Table 1). Acne lesions involve inflammation, an anti-acne formulation must possess this activity to reduce the inflammation [5]. Reduced inflammation can be due to the improved penetration profile of the K-EGF suggesting K-EGF as an effective treatment option for acne vulgaris.

## Anti-acne activity (on sebaceous glands)

Histopathological investigation of the excised skin from the interscapular region was performed to evaluate the anti-acne effect. Sections from skin of the normal (group 1), toxic (group 2), Std. allopathic gel (group 3), Std. herbal (group 4)- and K-EGF (group 5)-treated groups were examined for the change in size and number of sebaceous gland (SG) units in the dermis (Fig. 7). An increase in the number and size of SG unit was prominent in group 2 animals. Testosterone administration over several days produce enlargement of the SGs (Kausar et al. 2019). However, the animals subjected to acne treatments showed decrease in the number and size of the SG units. Group 3 (Std. allopathic gel) rats produced a decrease in number of SG units but not in size. However, the Std. herbal (Group 4)- and K-EGF (Group 5)-treated animals exhibited a slight decrease in both the number and size of the SG units, the result being more pronounced in case of K-EGF treatment and in sync with earlier report (Kausar et al. 2019). It has been also reported that reduction in SG size suppresses the production of sebum followed by inhibition of sebocyte differentiation which is a benchmark in acne treatment (Orfanos et al. 1997).

Table 1 Effect of topical administration of Anti-acne ethosomal gel (K-EGF), standard herbal and standard allopathic gel on Carrageenan-induced rat paw edema

Group	Treatment	Paw volume (mm) (Mean ± S.D.)				% Inhibition
		Initial	1 h	2 h	3 h	
Normal Control	–	1.09 ± 0.04	1.11 ± 0.04	1.18 ± 0.03	1.14 ± 0.05	–
Toxic Control	CGN* + Blank-EGF	1.32 ± 0.05[†]	1.45 ± 0.05[†]	1.56 ± 0.03[†]	1.59 ± 0.03[†]	–
Standard Allopathic Gel	CGN* + Clindac A Gel	1.23 ± 0.06*	1.42 ± 0.02*	1.38 ± 0.04*	1.31 ± 0.05**	70.37%
K-EGF	CGN* + K-EGF	1.16 ± 0.05**	1.39 ± 0.03*	1.33 ± 0.02**	1.25 ± 0.06**	66.66%

(All values are reported as mean ± S.D., [†]$p < 0.01$ vs normal control, *$p < 0.05$ vs toxic control, **$p < 0.01$ vs toxic control)
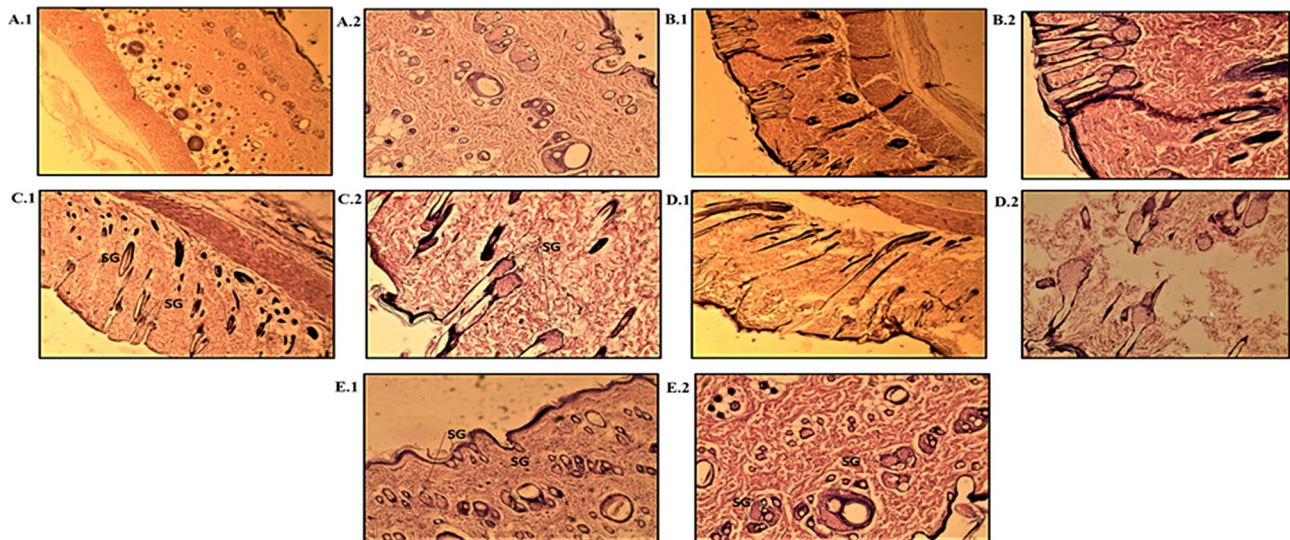
Fig. 7 Histopathological evaluation of control and different formulations; (Group 1) control—low power (10X) (**A1**) and high power (40X) (**A2**) photomicrograph; (Group 2) toxic—low power (10X) photomicrograph (**B1**) and High power (40X) photomicrograph (**B2**); (Group 3) standard allopathic gel—low power (10X) photomicrograph (**C1**) and high power (40X) photomicrograph (**C2**); (Group 4) herbal standard—low power (10X) photomicrograph (**D1**) and high power (40X) photomicrograph (**D2**); (Group 5) K-EGF—low power (10X) photomicrograph (**E1**) and high power (40X) photomicrograph (**E2**)

Accelerated stability studies

On storage of anti-acne ethosomal gel samples at 40 ± 2 °C and $75 \pm 5\%$ RH for a period of 3 months, the appearance of the formulations was clear with no significant variation in pH and drug content. The presence of ethanol as a chief constituent in the ethosomes imparts it a net negative surface charge that avoids vesicular aggregation due to electrostatic repulsion (Verma and Pathak, 2012). This indicates sufficient stability of the developed ethosomal gel.

Conclusion

The present investigation verified that the nano-sized flexible ethosomal vesicles acted as efficient carrier for the delivery of karanjin to the deeper layers of the skin. Dynamic light scattering, electron microscopy, entrapment efficiency and permeation experiments showed favorable results for incorporation of ethosomes into the gel bases. Further, characterization of the developed ethosomal gel revealed physicochemical properties acceptable for dermal delivery of the therapeutic agent. The antibacterial evaluation in the acne causing bacteria and the antioxidant evaluation depicted improved effects with the ethosomal formulation. The *in-vivo* evaluations confirmed the effectiveness of the anti-inflammatory and anti-acne properties of the karanjin-loaded ethosomal gel.

Declarations

References

Abdulbaqi I, Darwis Y, Khan AK et al (2016) Ethosomal nanocarriers: the impact of constituents and formulation techniques on ethosomal properties, in vivo studies, and clinical trials. IJN. https://doi.org/10.2147/IJN.S105016

Ahmed TA (2015) Preparation of transfersomes encapsulating sildenafil aimed for transdermal drug delivery: Plackett-Burman design and characterization. J Liposome Res 25:1–10. https://doi.org/10.3109/08982104.2014.950276

Arora MK, Yadav A, Saini V (2011) Role of hormones in acne vulgaris. Clin Biochem 44:1035–1040. https://doi.org/10.1016/j.clinbiochem.2011.06.984

Arshad N, Rashid N, Absar S, Abbasi M, Saleem S, Mirza B (2013) UV-absorption studies of interaction of karanjin and karanjachromene with ds. DNA: evaluation of binding and antioxidant activity. Open Chem 11:2040–2047

Azimi H, Fallah-Tafti M, Khakshur AA, Abdollahi M (2012) A review of phytotherapy of acne vulgaris: perspective of new pharmacological treatments. Fitoterapia 83:1306–1317

Bragagni M, Mennini N, Maestrelli F, Cirri M, Mura P (2012) Comparative study of liposomes, transfersomes and ethosomes as carriers for improving topical delivery of celecoxib. J Drug Deliv 19:354–361

Chandrasekar D, Madhusudhana K, Ramakrishna S, Diwan PV (2006) Determination of DPPH free radical scavenging activity by reversed-phase HPLC: a sensitive screening method for polyherbal formulations. J Pharm Biomed 40:460–464

Chin JM, Goldstein DB (1997) Membrane disordering action of ethanol: variation with membrane cholesterol content and depth of the spin label probe. Mol Pharmacol 13:435–441

Chomnawang MT, Surassmo S, Nukoolkarn VS, Gritsanapan W (2005) Antimicrobial effects of Thai medicinal plants against acne-inducing bacteria. J Ethnopharmacol 101:330–333

Cong T-X, Hao D, Wen X, Li X-H, He G, Jiang X (2019) From pathogenesis of acne vulgaris to anti-acne agents. Arch Dermatol Res 311:337–349. https://doi.org/10.1007/s00403-019-01908-x

Draize JH (1944) Methods for the study of irritation and toxicity of substances applied topically to the skin and mucous membranes. J Pharmacol Exp Ther 82:377–390

Dreno B (2004) Topical antibacterial therapy for acne vulgaris. Drugs 64:2389–2397. https://doi.org/10.2165/00003495-200464210-00002

Dubey V, Mishra D, Dutta T, Nahar M, Saraf D, Jain N (2007) Dermal and transdermal delivery of an anti-psoriatic agent via ethanolic liposomes. J Control Release 123:148–154

Fang J-Y, Sung K, Lin H-H, Fang C-L (1999) Transdermal iontophoretic delivery of diclofenac sodium from various polymer formulations: in vitro and in vivo studies. Int J Pharm 178:83–92

Fang YP, Tsai YH, Wu PC, Huang YB (2008) Comparison of 5-aminolevulinic acid-encapsulated liposome versus ethosome for skin delivery for photodynamic therapy. Int J Pharm 356:144–152

Fox L, Csongradi C, Aucamp M, du Plessis J, Gerber M (2016) Treatment modalities for acne. Molecules 21:1063. https://doi.org/10.3390/molecules21081063

Garg BJ, Garg NK, Beg S, Singh B, Katare OP (2016) Nanosized ethosomes-based hydrogel formulations of methoxsalen for enhanced topical delivery against vitiligo: formulation optimization, in vitro evaluation and preclinical assessment. J Drug Target 24:233–246. https://doi.org/10.3109/1061186X.2015.1070855

Garg V, Singh H, Bhatia A, Raza K, Singh SK, Singh B, Beg S (2017) Systematic development of transethosomal gel system of piroxicam: formulation optimization, in vitro evaluation, and ex vivo assessment. AAPS Pharm Sci Tech 18:58–71. https://doi.org/10.1208/s12249-016-0489-z

Ghosh A, Tiwari GJ (2018) Role of nitric oxide-scavenging activity of Karanjin and Pongapin in the treatment of Psoriasis. 3 Biotech 8:338

Godin B, Touitou E (2004) Mechanism of bacitracin permeation enhancement through the skin and cellular membranes from an ethosomal carrier. J Control Release 94:365–379

Gollnick H, Cunliffe W, Berson D et al (2003) Management of Acne. JAAD 49:S1–S37. https://doi.org/10.1067/mjd.2003.618

Heng AHS, Chew FT (2020) Systematic review of the epidemiology of acne vulgaris. Sci Rep 10:5754. https://doi.org/10.1038/s41598-020-62715-3

Horita D, Hatta I, Yoshimoto M, Kitao Y, Todo H, Sugibayashi K (2015) Molecular mechanisms of action of different concentrations of ethanol in water on ordered structures of intercellular lipids and soft keratin in the stratum corneum. Biochim Biophys Acta Biomembr 1848:1196–1202. https://doi.org/10.1016/j.bbamem.2015.02.008

Hurler J, Engesland A, Poorahmary KB, Škalko-Basnet N (2012) Improved texture analysis for hydrogel characterization: gel cohesiveness, adhesiveness, and hardness. J Appl Polym Sci 125:180–188. https://doi.org/10.1002/app.35414

Ibrahim TM, Abdallah MH, El-Megrab NA, El-Nahas HM (2019) Transdermal ethosomal gel nanocarriers; a promising strategy for enhancement of anti-hypertensive effect of carvedilol. J Liposome Res 29:215–228. https://doi.org/10.1080/08982104.2018.1529793

International Conference on Harmonization (2003) Q1A (R2), Stability testing of new drug substances and products. In: Presented at the International Conference on Harmonization. International Conference on Harmonization Geneva

Kahraman E, Güngör S, Özsoy Y (2017) Potential enhancement and targeting strategies of polymeric and lipid-based nanocarriers in dermal drug delivery. Ther Del 8:967–985. https://doi.org/10.4155/tde-2017-0075

Kausar H, Mujeeb M, Ahad A, Moolakkadath T, Aqil M, Ahmad A, Akhter MH (2019) Optimization of ethosomes for topical thymoquinone delivery for the treatment of skin acne. J Drug Deliv Sci Technol 49:177–187. https://doi.org/10.1016/j.jddst.2018.11.016

Kumar A, Baboota S, Agarwal S, Ali J, Ahuja A (2008) Treatment of acne with special emphasis on herbal remedies. Exp Rev Dermat 3:111–122. https://doi.org/10.1586/17469872.3.1.111

Kumar B, Pathak R, Mary PB, Jha D, Sardana K, Gautam HK (2016) New insights into acne pathogenesis: Exploring the role of acne-associated microbial populations. Dermatol Sin 34:67–73. https://doi.org/10.1016/j.dsi.2015.12.004

Negi LM, Jaggi M, Talegaonkar S (2013) A logical approach to optimize the nanostructured lipid carrier system of irinotecan: efficient hybrid design methodology. Nanotechnology 24:015104. https://doi.org/10.1088/0957-4484/24/1/015104

Orfanos CE, Zouboulis ChC, Almond-Roesler B et al (1997) Current use and future potential role of retinoids in dermatology. Drugs 53:358–388

Patel PP, Trivedi ND (2012) Karanjin ameliorates DSS induced colitis in C57BL/6 mice. Int J Pharm Sci Res 6:4866–4874

Rani MS, Dayanand C, Shetty J, Vegi PK, Kutty AM (2013) Evaluation of antibacterial activity of pongamia pinnata linn on pathogens of clinical isolates. Am J Phytomed Clin Ther 1:645–651

Ravikumar V, Khan MS, Kumar MM (2011) Development of RP-HPLC method for the quantification of karanjin in the seeds extracts of Pongamia glabra. Int J Pharm Tech 3:1433–1448

Remington JP (2006) Remington: the science and practice of pharmacy. Lippincott Williams & Wilkins, Philadelphia

Shahtalebi M, Asghari G, Rahmani F, Shafiee F, Jahanian-Najafabadi A (2018) Formulation of herbal gel of *Antirrhinum majus* extract and evaluation of its anti-propionibacterium acne effects. Adv Biomed Res 7:53. https://doi.org/10.4103/abr.abr_99_17

Shejawal N, Menon S, Shailajan S (2014) Bioavailability of karanjin from *Pongamia pinnata* L. in Sprague dawley rats using validated RP-HPLC method. J App Pharm Sci 4:10–14

Singh R, Pandey B (1996) Anti-Inflammatory activity of seed extracts of *Ponamia pinnata* in Rat. Ind J Phys Pharmacol 40:355–358

Singh A, Jahan I, Sharma M, Rangan L, Khare A, Panda AN (2016) Structural characterization, in silico studies and in vitro antibacterial evaluation of a furanoflavonoid from karanj. Planta Medica Let 3:e91–e95

Srinivasan K, Muruganandan S, Lal J et al (2001) Evaluation of anti-inflammatory activity of *Pongamia pinnata* leaves in rats. J Ethnopharmacol 78:151–157. https://doi.org/10.1016/S0378-8741(01)00333-6

Tanghetti EA (2013) The role of inflammation in the pathology of acne. J Clin Aesthetic Dermat 6:27

Touitou E, Dayan N, Bergelson L, Godin B, Eliaz M (2000) Ethosomes; novel vesicular carriers for enhanced delivery: characterization and skin penetration properties. J Control Release 65:403–418

Ujwal P, Kumar M, Naika HR, Hosetti B (2007) Antimicrobial activity of different extracts of *Pongamia pinnata*. Med Aromat Plant Sci Biotechnol 1:285–287

Verma P, Pathak K (2012) Nanosized ethanolic vesicles loaded with econazole nitrate for the treatment of deep fungal infections through topical gel formulation. Nanomedicine 8:489–496. https://doi.org/10.1016/j.nano.2011.07.004

Wong A, Zhang B, Jiang M, Gong E, Zhang Y, Lee S (2016) Oxidative stress in acne vulgaris. J Clin Dermatol Ther 3:020

Yang L, Wu L, Wu D, Shi D, Wang T, Zhu X (2017) Mechanism of transdermal permeation promotion of lipophilic drugs by ethosomes. IJN 12:3357–3364. https://doi.org/10.2147/IJN.S134708

Yang JH, Hwang EJ, Moon J et al (2019) Clinical efficacy of herbal extracts in treatment of mild to moderate acne vulgaris: an 8-week, double-blinded, randomized, controlled trial. J Dermatol Treat 16:1–5. https://doi.org/10.1080/09546634.2019.1657792

Yeşilada E, Küpeli E (2002) Berberis crataegina DC. root exhibits potent anti-inflammatory, analgesic and febrifuge effects in mice and rats. J Ethnopharmacol 79:237–248

Yi D, Wang Z, Yi L (2015) Development and validation of an LC-MS method for determination of karanjin in rat plasma: application to preclinical pharmacokinetics. J Chromatogr Sci 53:456–461. https://doi.org/10.1093/chromsci/bmu064

Yu Z, Lv H, Han G, Ma K (2016) Ethosomes loaded with cryptotanshinone for acne treatment through topical gel formulation. PLoS ONE 11:e0159967. https://doi.org/10.1371/journal.pone.0159967